

A.K. S. Poli¹, R. B. Hilário¹, A. M. Gama², M. Baldan^{1,3}, E. S. Gonçalves^{1,2}

¹Instituto Tecnológico da Aeronáutica, São José dos Campos, SP, Brasil.

²Instituto de Aeronáutica e Espaço, Laboratório de Caracterização Físico-Química, Divisão de Materiais, São José dos Campos, SP, Brasil.

³Instituto Nacional de Pesquisas Espaciais, Laboratório Associado de Sensores, São José dos Campos, SP, Brasil.

karoline-poli@hotmail.com

ABSTRACT

Supercapacitors have been applied in several fields such as portable electronics, hybrid electric vehicle and so on. Carbon-based materials and conducting polymers are described as effective to play this role. The polyaniline (PANI) deserves attention due to its capacity to store energy, ease of handling, low cost and high conductivity. The carbon fiber felt presents high specific surface area, low specific mass and relative stability to chemical attack. When combined, PANI and CFF have peculiar characteristics due to the synergism between these materials, since the electroactive character of the polymer is added to the large surface area and its physical-chemical stability of felt

EXPERIMENTAL SECTION

Carbon Fiber Felt
(1400, 1600, 2000 and 2300K)

Polymerization
cyclic applications from -0,50 V to +1,05 V vs Ag/AgCl, em 25 mVs⁻¹

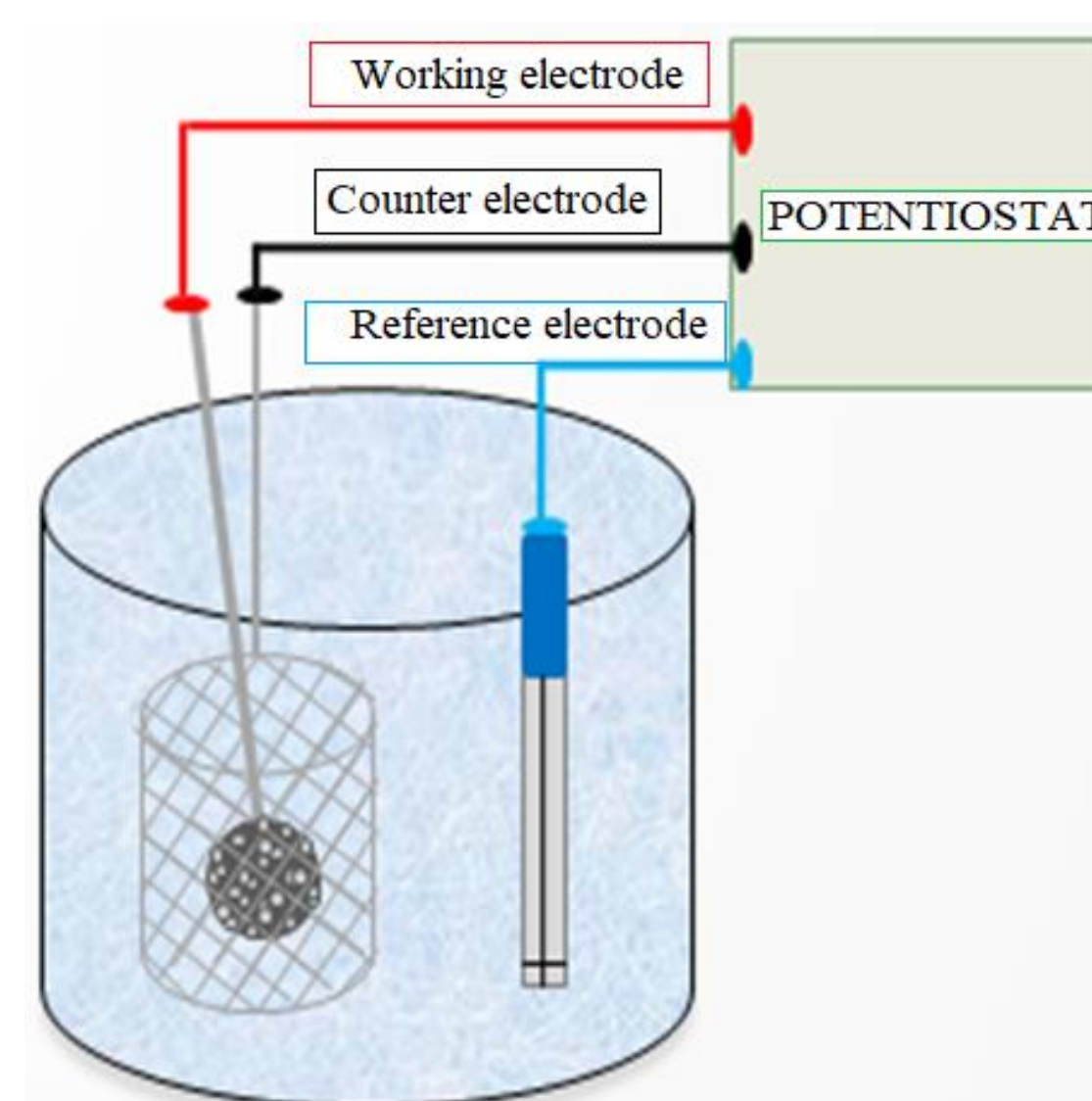
0,1mol⁻¹ aniline and 0,5 molL⁻¹ H₂SO₄

PANI@CFF

morphological characterization

electrochemical characterization

Structural characterization



RESULTS AND DISCUSSION

Characterization of Carbon Fiber Felt

Scanning Electron Microscopy

X-ray Diffraction patterns

The stacking size of the lamellar planes, the interplanar distance between them and the crystallite size can be calculated according to Equations 1, 2 and 3, respectively

$$\text{Equation 1: } L_{002} = \frac{0.89 \lambda}{W_{1/2} \cos \theta}$$

$$\text{Equation 2: } d_{002} = \frac{\lambda}{2 \sin \theta}$$

$$\text{Equation 3: } L_a = \frac{1.84 \lambda}{W_{1/2} \cos \theta}$$

Table 1. Stacking size of the lamellar planes, interplanar distance and crystallite size.

CFF (K)	1400	1600	2000	2300
L_{002} (nm)	1.532	1.655	2.135	3.159
d_{002} (nm)	0.354	0.353	0.349	0.345
L_a (nm)	4.50	4.60	6.59	7.75

Raman Scattering Spectroscopy

The equation 4 was used to determine the size of the crystallites (L_a)

$$\text{Equation 4: } L_a = 4.4 \left(\frac{I_G}{I_{D1}} \right)$$

Table 2. Main Raman bands of CFF.

CFF (K)	I_{D1}/I_G	I_{D3}/I_G	L_a (nm)
1400	1.67	0.49	2.64
1600	1.44	0.33	3.06
2000	1.25	0.10	3.52
2300	1.09	0.06	4.05

Table 3. Electrical phenomena obtained from EIS circuit fit of CFF

CFF (K)	1400	1600	2000	2300
R_2 (Ω)	6.62	1.16×10^5	1.69×10^5	1.92×10^5
C_2 (μ F)	1.25×10^3	491	274	899
R_3 (Ω)	---	5.74	4.22	4.55×10^3
C_3 (μ F)	---	376	391	2.92×10^3

Characterization of PANI@CFF composites

Polarographic Data

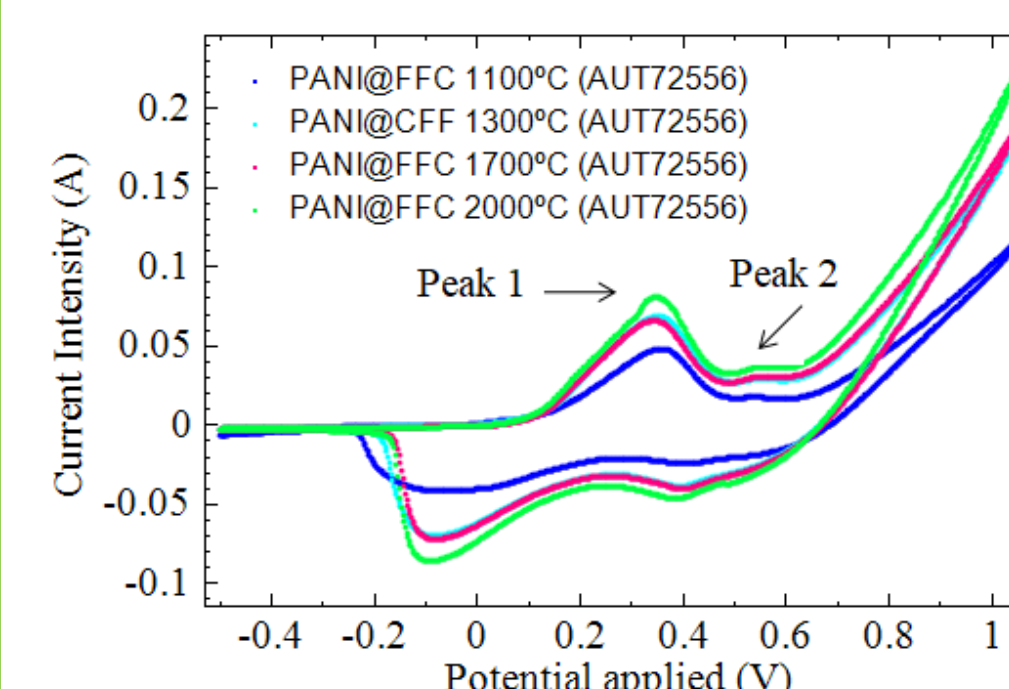


Figure 6: Polarographic data obtained during carbon g electro-synthesis of polyaniline on fiber felt as substrate.

CFF (K)	Potential 1 (V)	Current 1 (A)	Potential 2 (V)	Current 2 (A)
1400	0.351	0.038	0.539	6.606×10^{-4}
1600	0.341	0.050	0.544	1.609×10^{-3}
2000	0.344	0.049	0.546	1.478×10^{-3}
2300	0.339	0.059	0.544	2.266×10^{-3}

Scanning Electron Microscopy

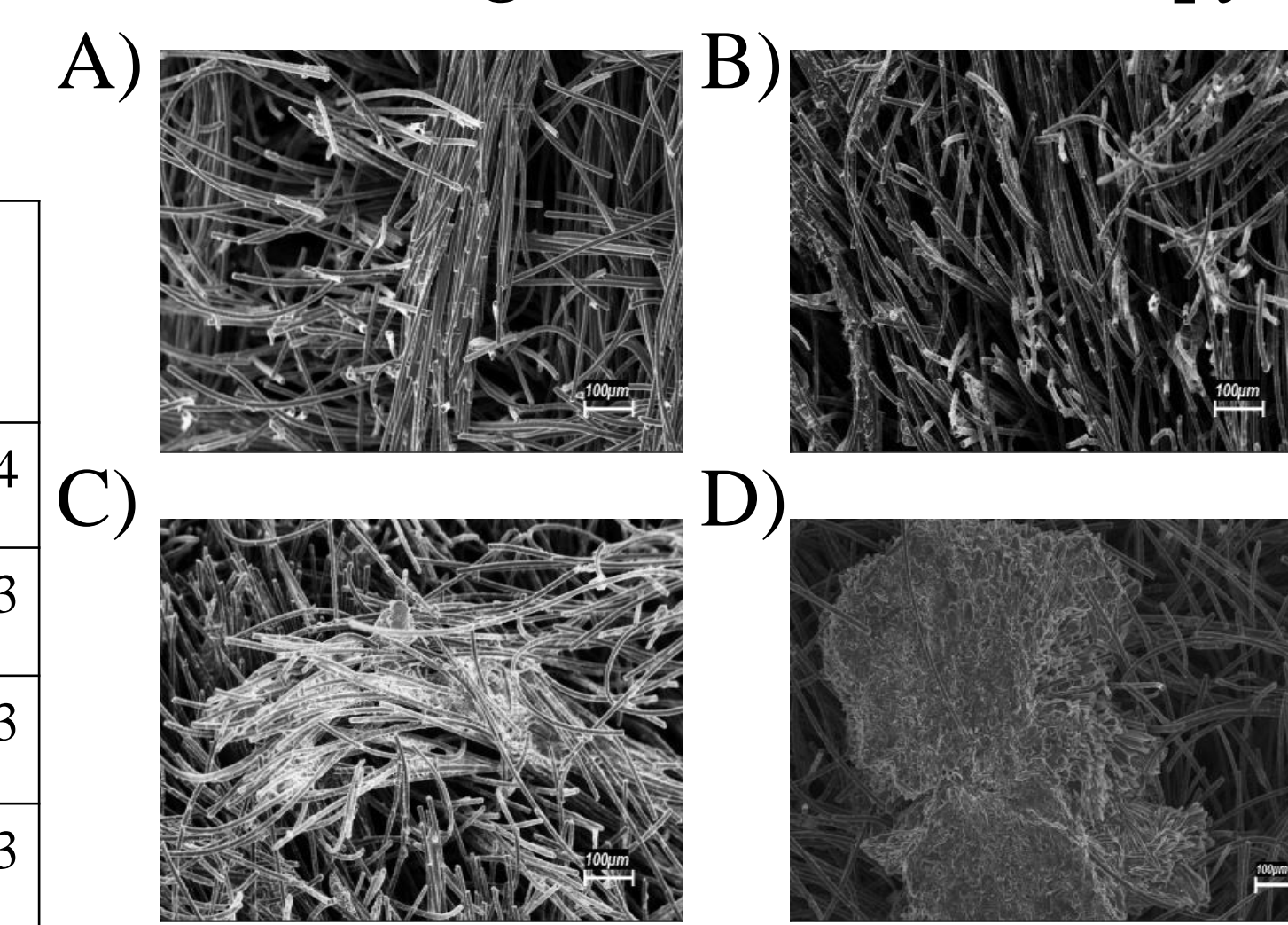


Figure 7. SEM images of polyaniline@carbon fiber felts composites, PANI@CFF, at a) 1400K, b) 1600K, c) 2000K and d) 2300K.

X-ray Diffraction patterns

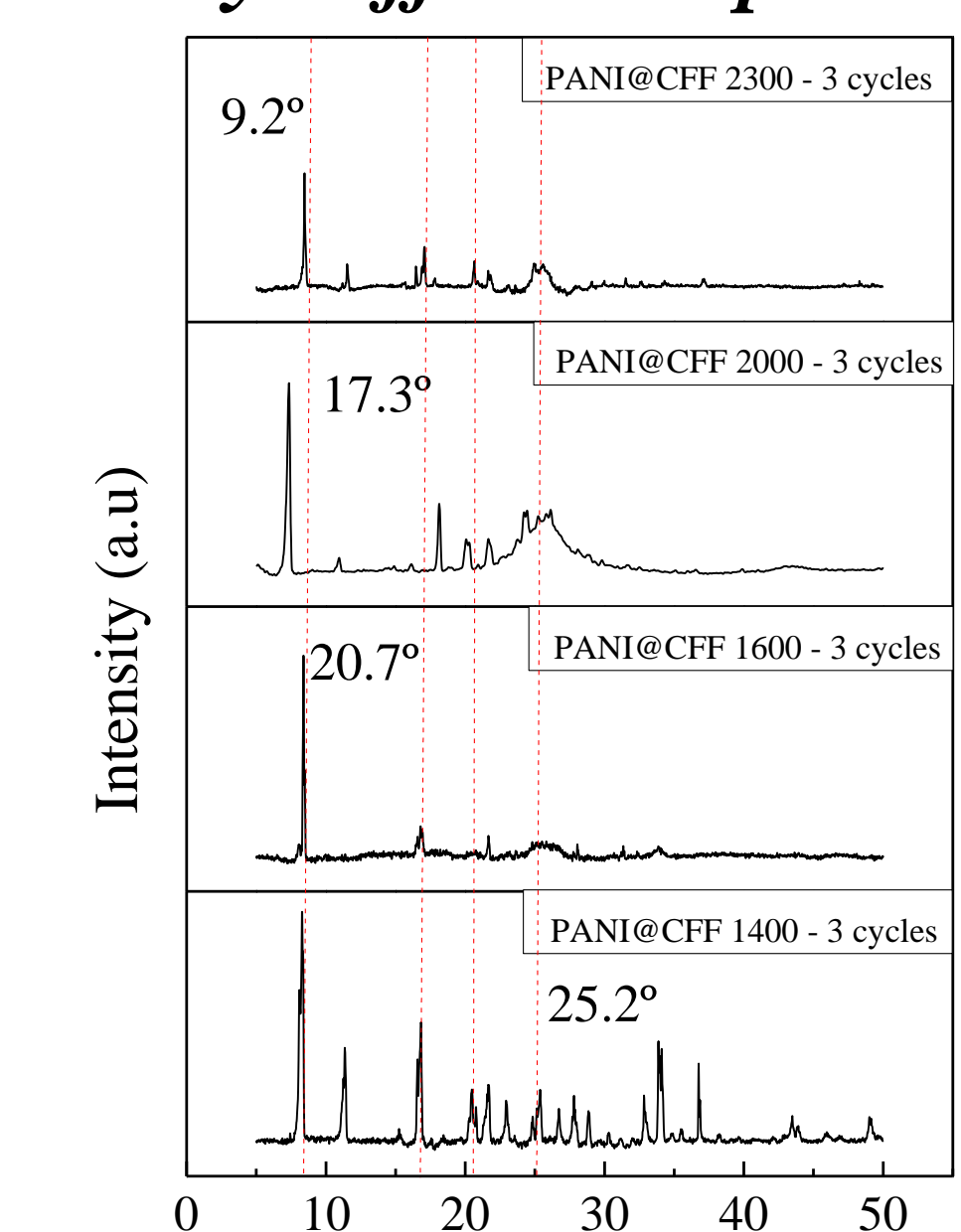


Figure 8. X-ray diffraction of PANI@CFF composites at a) 1400K, b) 1600K, c) 2000K and d) 2300K.

Raman Scattering Spectroscopy

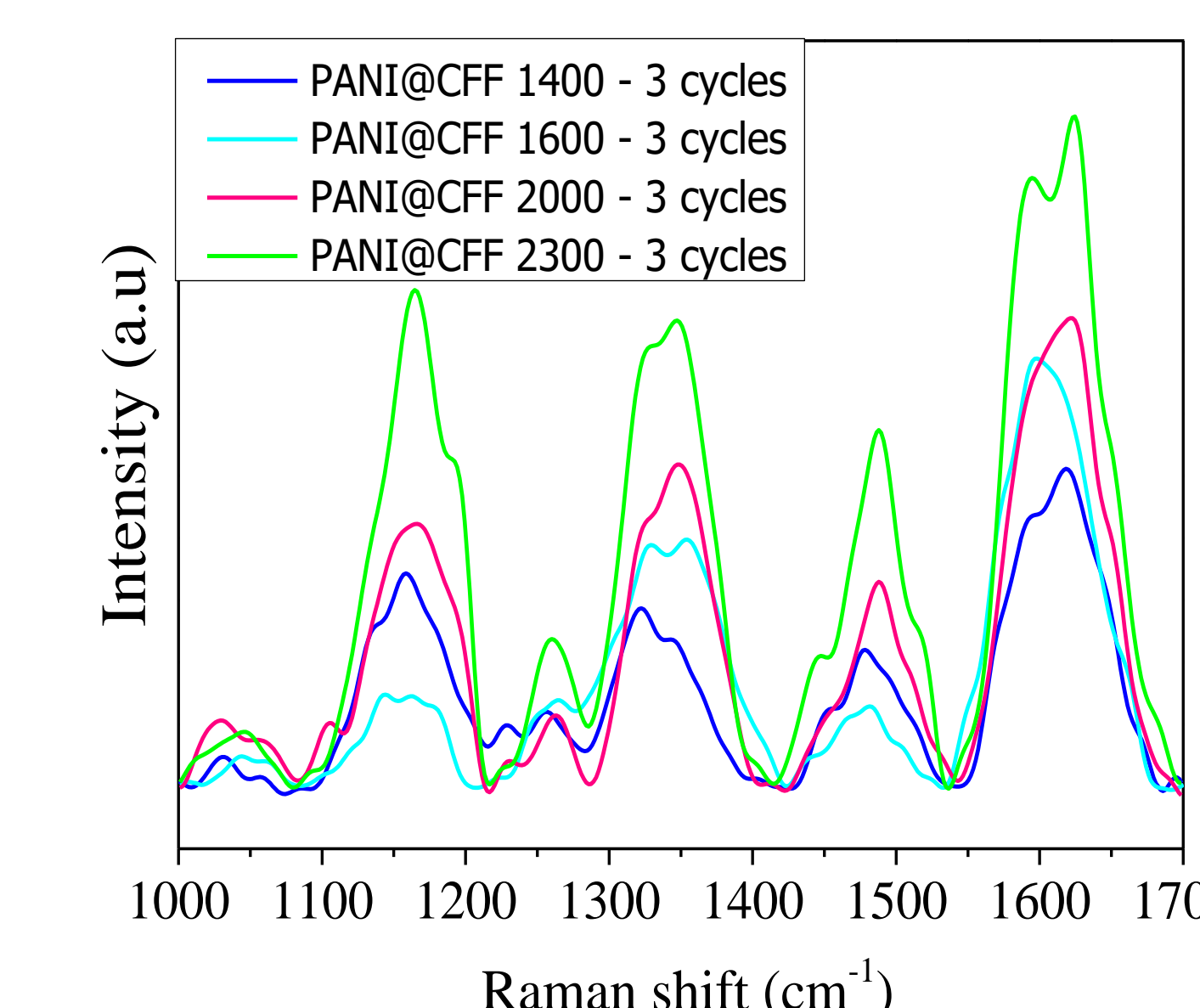


Figure 9. Raman Spectroscopy of PANI@CFF composites at a) 1400K, b) 1600K, c) 2000K and d) 2300K.

From the Equations 5, 6, 7 and 8 was calculated the degree of oxidation, ratio of polar groups, mobile charges from bipolarons and conductivity index, respectively.

$$\text{Equation 5: } y = \frac{I_Q}{(I_Q + I_B)}$$

$$\text{Equation 6: } y_P = \frac{I_P}{(I_Q + I_B)}$$

$$\text{Equation 7: } y_{BP} = \frac{I_{BP}}{(I_Q + I_B)}$$

$$\text{Equation 8: } S = \frac{y_{BP}}{y_P}$$

Table 5. Oxidation, fixed and mobile charge ratios for PANI@CFF composites

CFF (K)	Cycles Number	y	y_P	y_{BP}	S
1400	3	0.45	0.53	0.06	0.121
1600		0.51	0.62	0.06	0.102
2000		0.48	0.90	0.16	0.176
2300		0.50	0.48	0.12	0.256

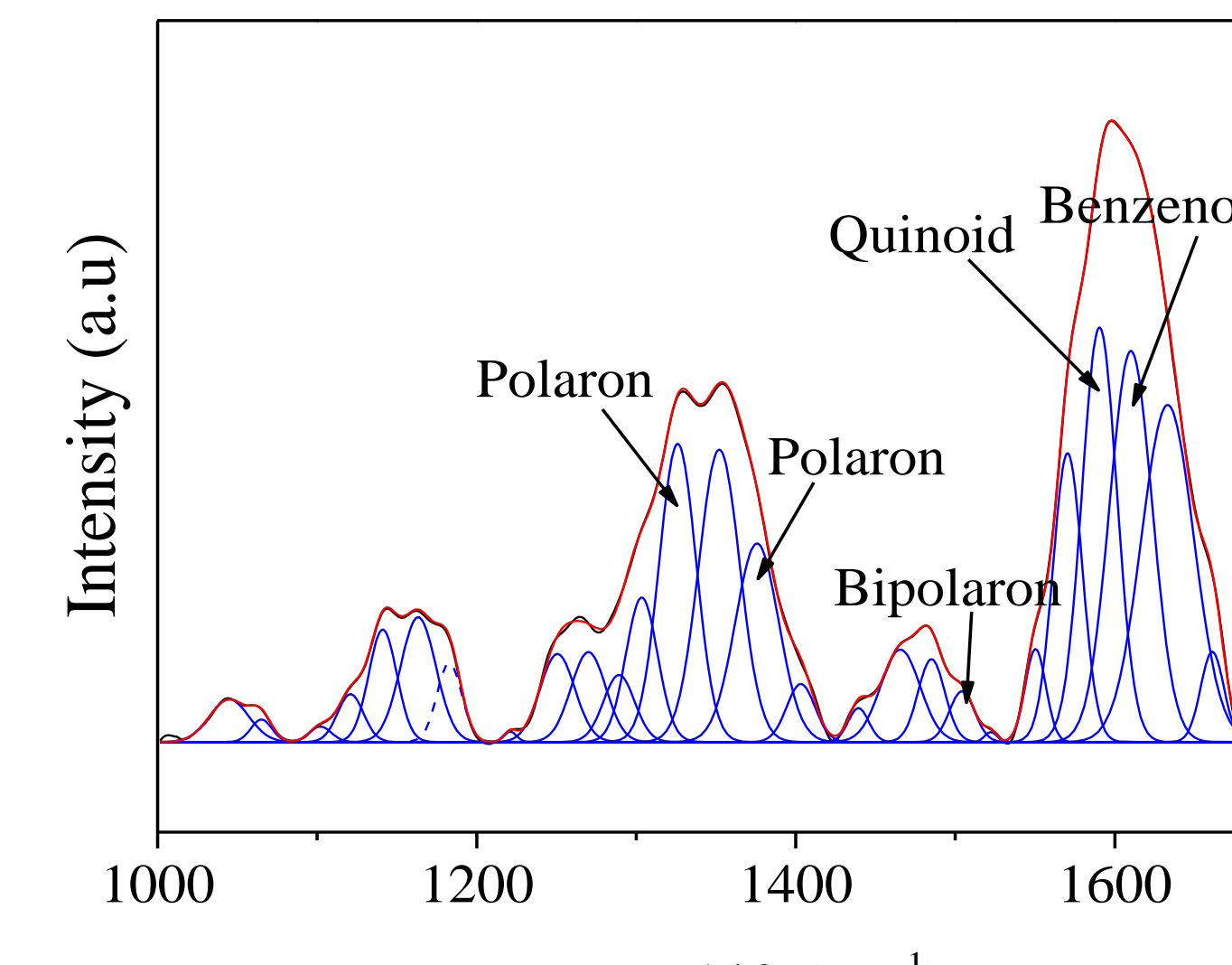


Figure 10. Raman Spectra fit of PANI@CFF composite at 1600K.

Electrochemical Impedance Spectroscopy

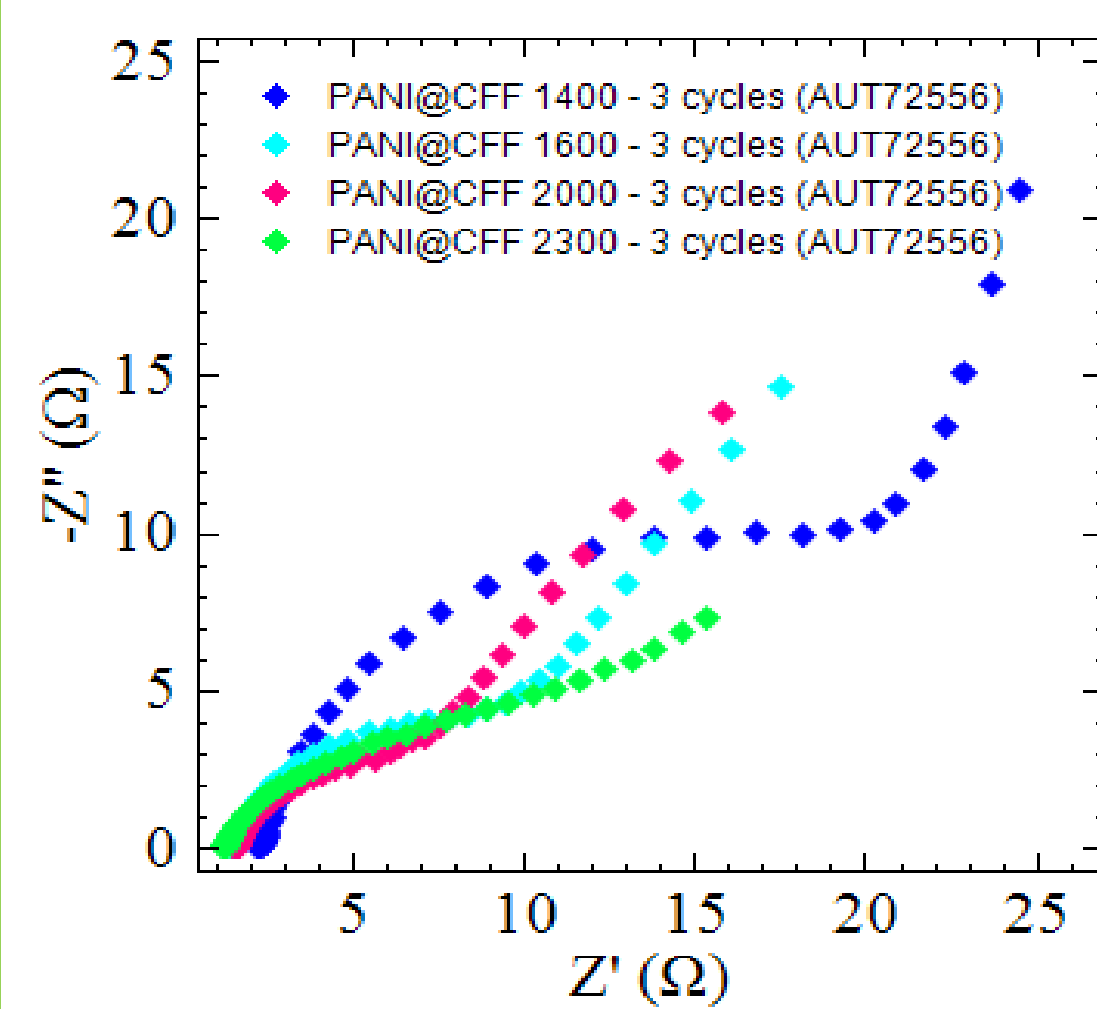


Figure 11. Electrochemical Impedance Spectroscopy of PANI@CFF composites.

Electrochemical Impedance Spectroscopy

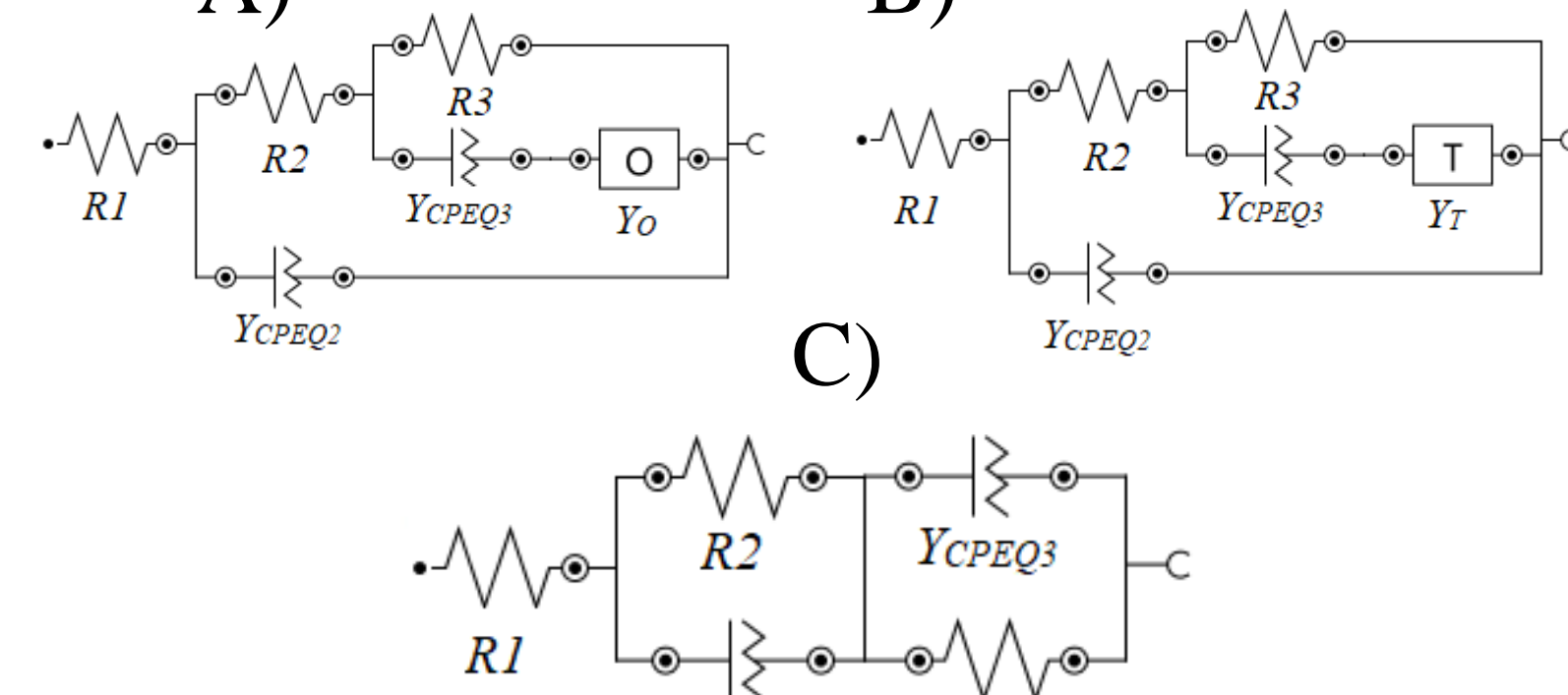


Figure 12. Electrical phenomena association fit of (A) PANI@CFF1400 and (B) PANI@CFF2000 and (C) PANI@CFF2300 obtained with 3 voltammetric cycles.

Table 6. Circuit elements obtained from IES circuit fit PANI@CFF composites

CFF (K)	1400	1600	2000	2300
R_2 (Ω)	25.2	9.50	6.33	5.90
C_2 (mF)	4.95	3.75	3.87	5.67
R_3 (Ω)	230	116	79.5	28.6
C_3 (mF)	73.1	160	144	140

CONCLUSIONS

The results shown that PANI@CFF2300, although it contains more agglomerates of PANI and even a lower proportion of protonated nitrogen atoms, had a higher mobility index, and the proportion of bipolarons (related to polarons) may be more relevant only to this surface. In the others, PANI@CFF1700 and PANI@CFF2000, the amount of PANI formed and its high crystalline orientation, in addition to the morphological regularity of the film, were decisive. Finally, the most effective precursor of a supercapacitive material was PANI@CFF2300, although the PANI@CFF2000 composite can not be completely discarded for this purpose.

ACKNOWLEDGEMENT



This study was financed in part by the Coordenação de Aperfeiçoamento de Pessoal de Nível Superior – Brasil (CAPES) - Finance Code 001

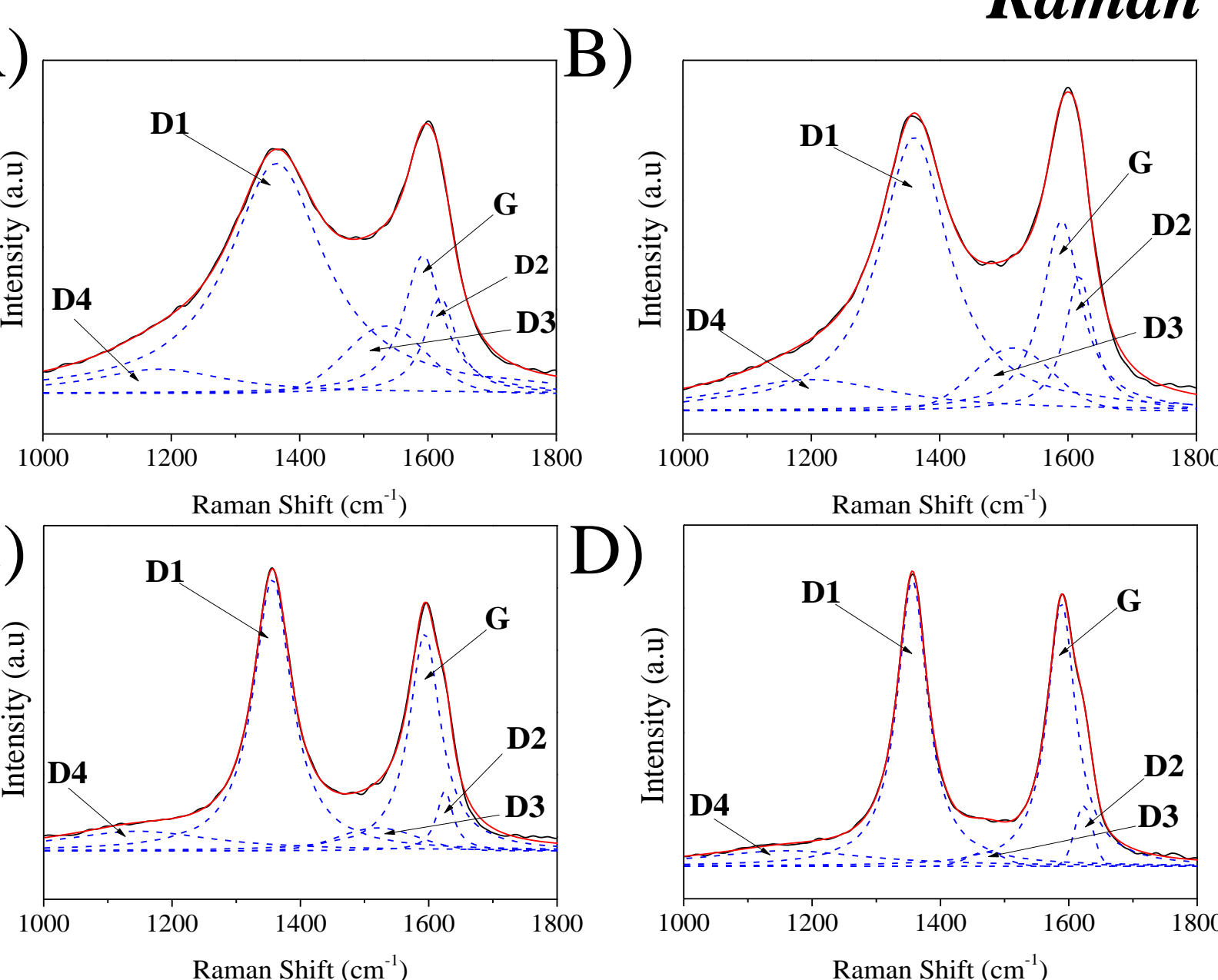


Figure 3. Raman spectra of CFF: A) 1400, B) 1600, C) 2000 and D) 2300K

Electrochemical Impedance Spectroscopy

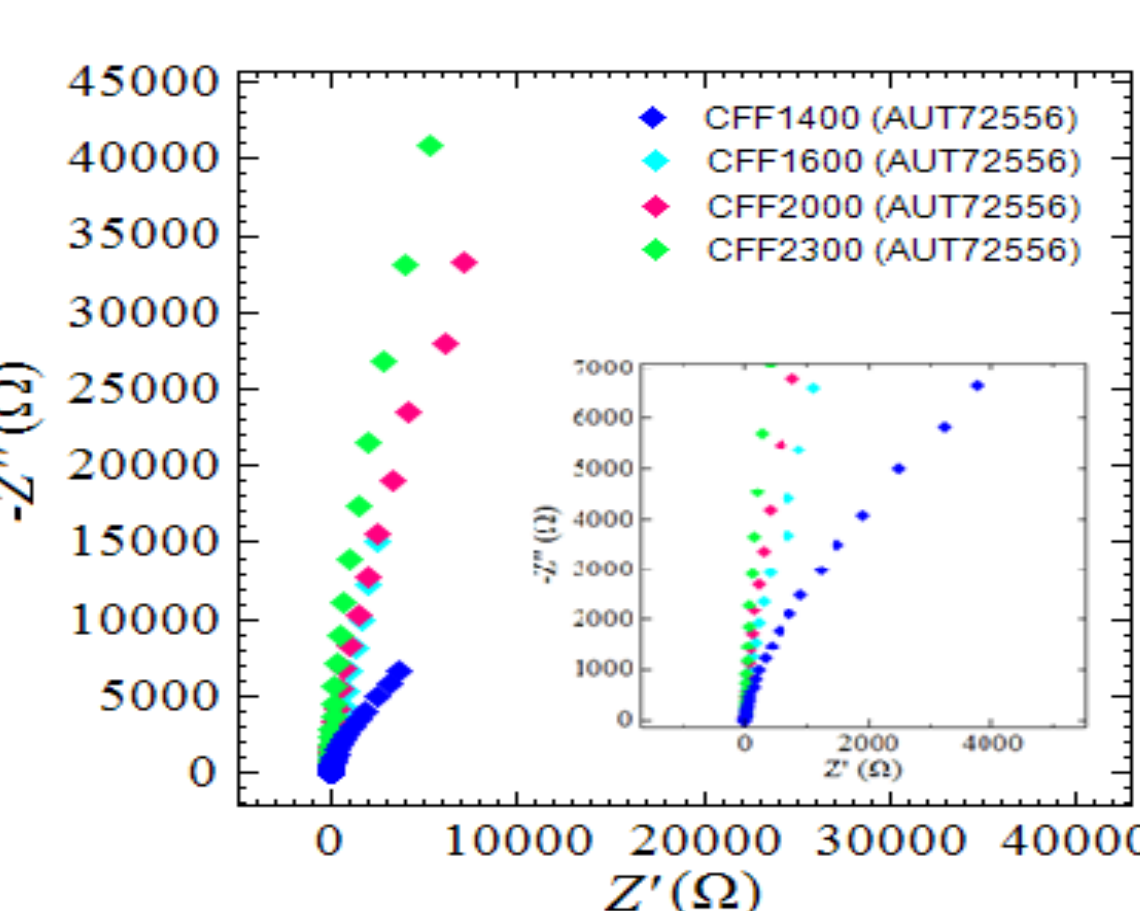


Figure 4. Electrochemical Impedance Spectra obtained for CFF1400, CFF1600, CFF2000 and CFF2300.

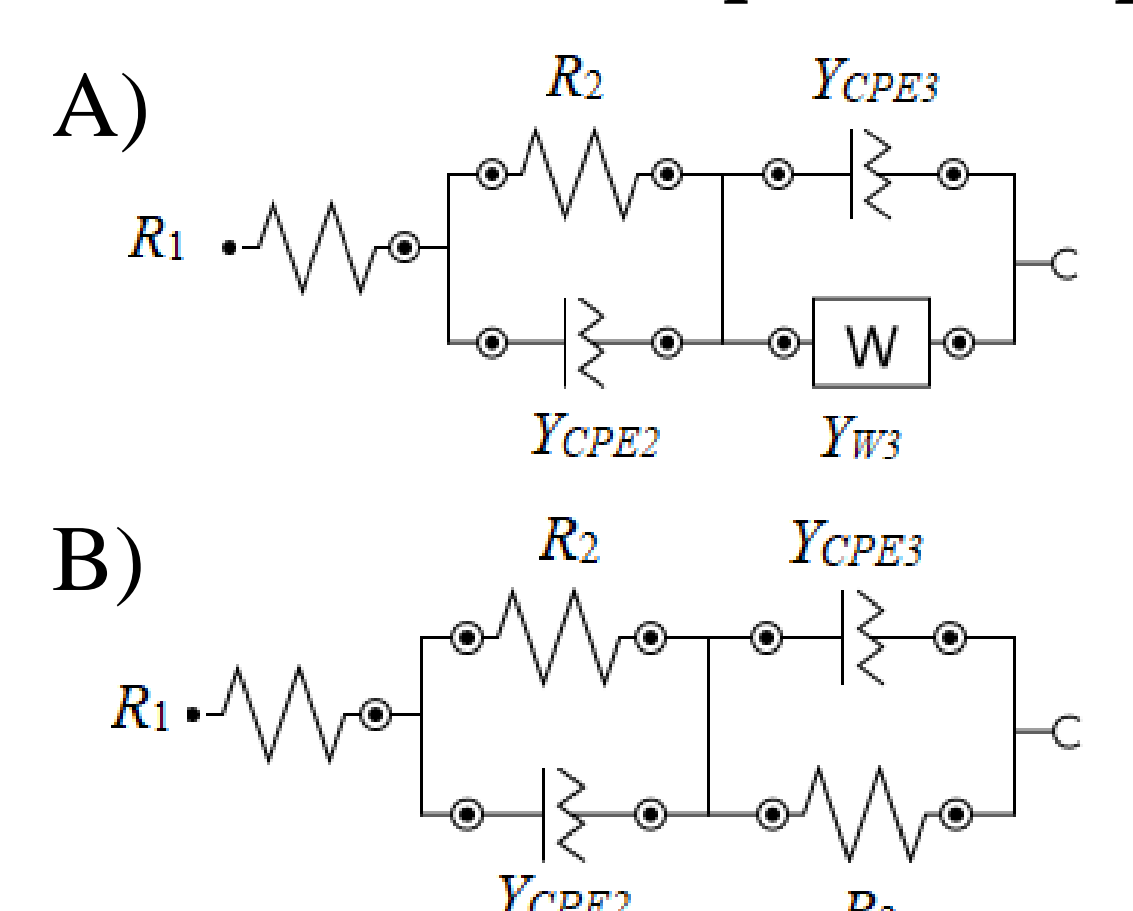


Figure 5. Association for the composite PANI@CFF1400 and b) 1600, 2000 and 2300K